

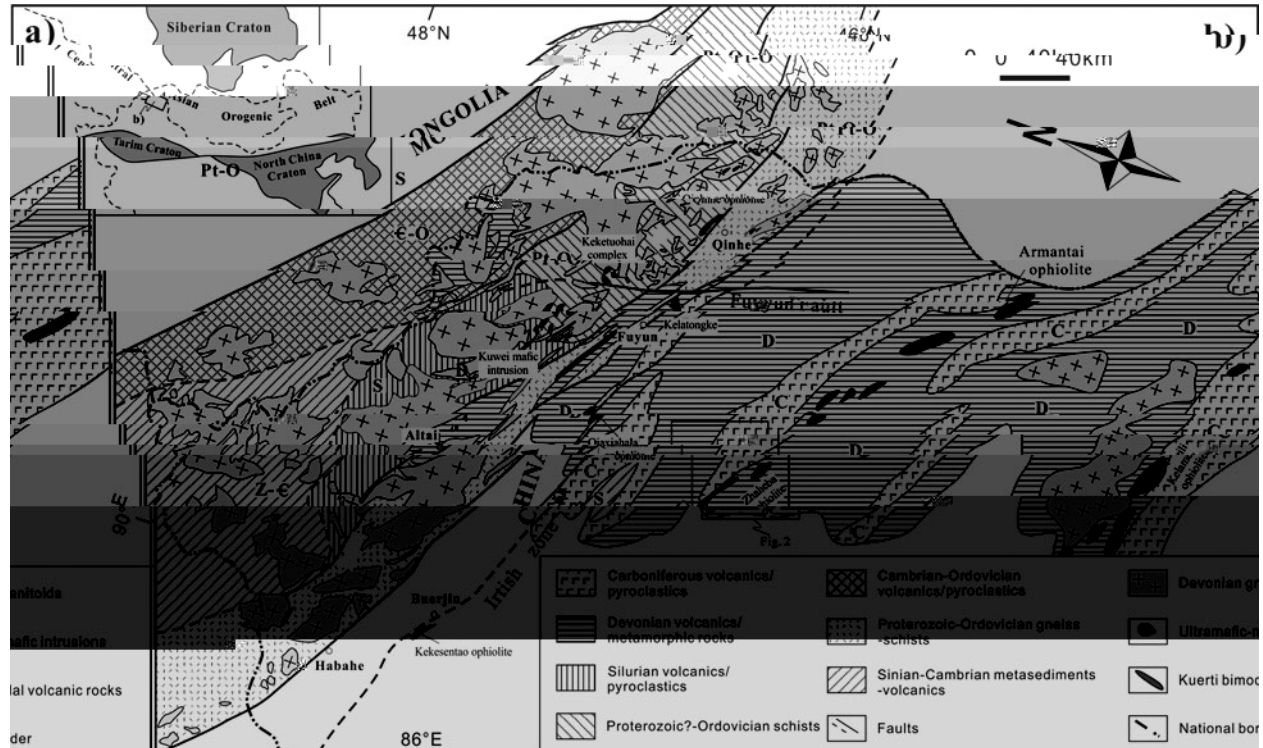
(Received 1 May 2015 accepted 10 January 2016 first published online 1 March 2016)

Abstract / *The tectonic evolution of the northern part of the North Anatolian Fault Zone (NAFZ) is studied by means of a detailed geological mapping and structural analysis of the Tunceli–Kırıkkale region. The NAFZ is a major active fault system in Turkey, which has been active since the Miocene. The region is characterized by a complex geological history, with multiple phases of magmatic activity, metamorphism, and tectonism. The geological mapping and structural analysis reveal the presence of various geological units, including metamorphic rocks, igneous rocks, and sedimentary rocks. The results show that the NAFZ has been active throughout the Miocene and has caused significant deformation and displacement of the crust. The study also highlights the importance of understanding the geological evolution of the NAFZ for predicting future seismic events and developing effective mitigation strategies.*

1. Introduction

The North Anatolian Fault Zone (NAFZ) is one of the most active and well-studied fault systems in the world (e.g., Gürer *et al.* 2000; Gürer & Güvenç, 2000; Gürer *et al.* 2012; Gürer & Güvenç, 2012; Gürer *et al.* 2013; Gürer & Güvenç, 2013; Gürer *et al.* 2014; Gürer *et al.* 2015; Gürer & Güvenç, 2015; Gürer *et al.* 2016). The NAFZ is a major active fault system in Turkey, which has been active since the Miocene. The region is characterized by a complex geological history, with multiple phases of magmatic activity, metamorphism, and tectonism. The geological mapping and structural analysis reveal the presence of various geological units, including metamorphic rocks, igneous rocks, and sedimentary rocks. The results show that the NAFZ has been active throughout the Miocene and has caused significant deformation and displacement of the crust. The study also highlights the importance of understanding the geological evolution of the NAFZ for predicting future seismic events and developing effective mitigation strategies.

The NAFZ is a major active fault system in Turkey, which has been active since the Miocene. The region is characterized by a complex geological history, with multiple phases of magmatic activity, metamorphism, and tectonism. The geological mapping and structural analysis reveal the presence of various geological units, including metamorphic rocks, igneous rocks, and sedimentary rocks. The results show that the NAFZ has been active throughout the Miocene and has caused significant deformation and displacement of the crust. The study also highlights the importance of understanding the geological evolution of the NAFZ for predicting future seismic events and developing effective mitigation strategies.



1. ()
et al. 200).

2. R a , b a a
t a
1, 2).
1, 2).
1, 2).
1, 2).
1, 2).
1, 2).

0%
(40.0%)
(30.50%)
(5.10%)
(4.3%).
1. ().
et al. 2013)
(15.0%)
(15.0%)
(1.2%).
1, 2).

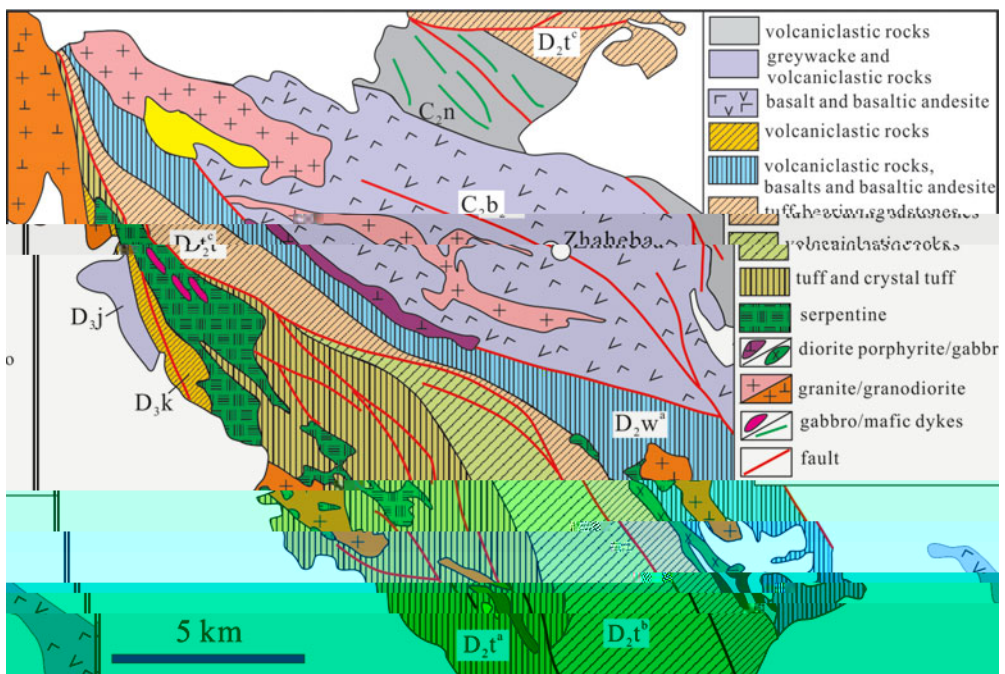


Fig. 2. (1) Geological cross-section of the Zhaheba ophiolite (modified after Li et al. 2005, 2006; see Fig. 1 for location); (2) field photographs of serpentinite (a) and serpentinized peridotite (b).

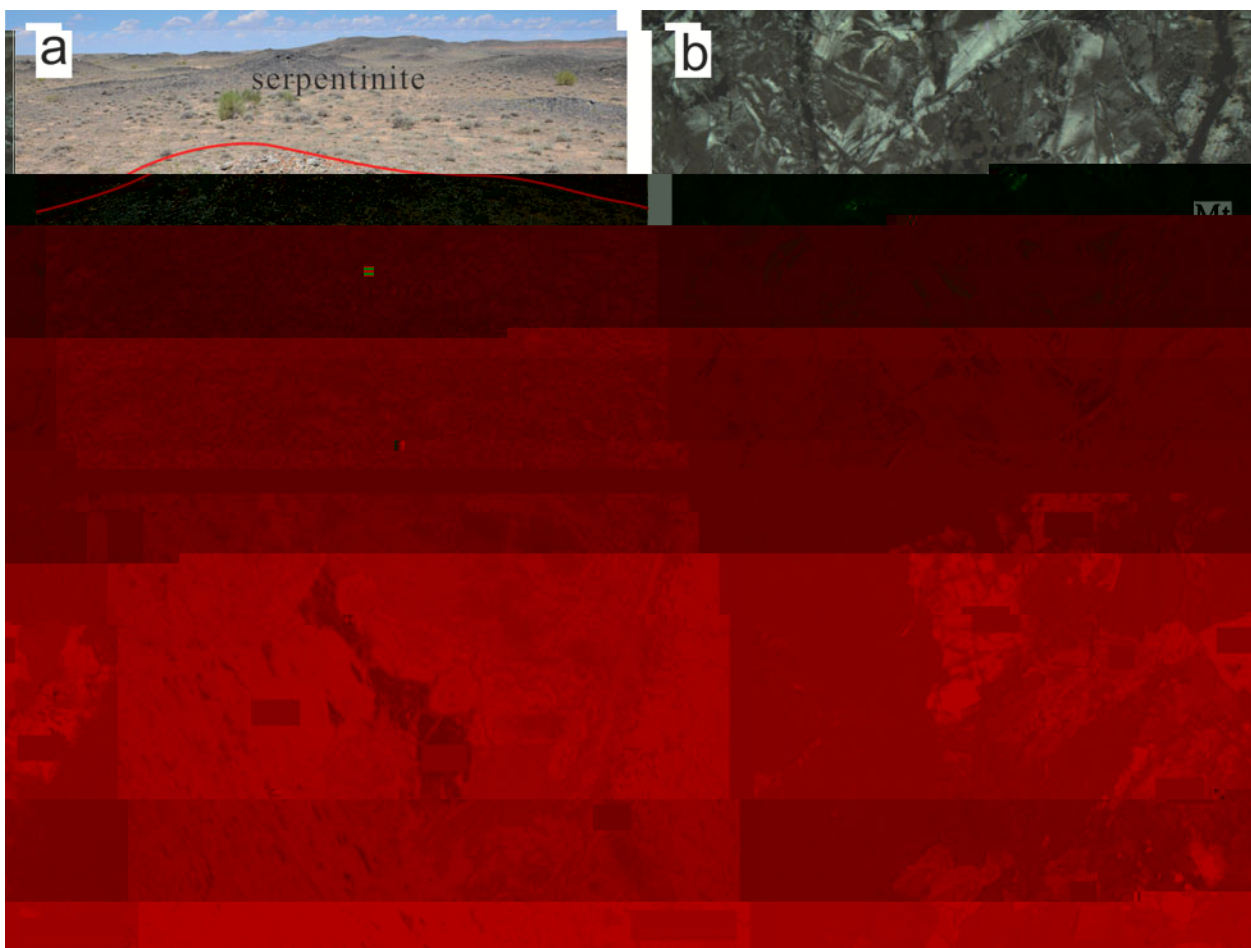


Fig. 3. (1) Geological cross-section of the Zhaheba ophiolite (modified after Li et al. 2005, 2006; see Fig. 1 for location); (2) field photographs of serpentinite (a) and serpentinized peridotite (b).

Geological setting and geological history of the study area

3. A a t e a l e

3.a. Z e c U Pb a a H r O t a a a

(2013) 01, 46°32'51" N, 24°2'4" E
 (2013) 02, 46°33'2" N, 24°2'36" E
 (2013) 03, 46°33'2" N, 24°2'36" E
 (2013) 04, 46°33'2" N, 24°2'36" E
 (2013) 05, 46°33'2" N, 24°2'36" E
 (2013) 06, 46°33'2" N, 24°2'36" E
 (2013) 07, 46°33'2" N, 24°2'36" E
 (2013) 08, 46°33'2" N, 24°2'36" E
 et al. (2011).
 et al. (2010).
 et al. (2003).

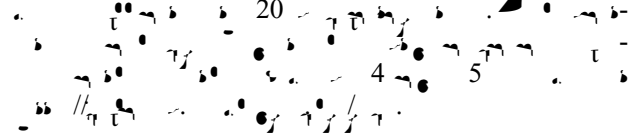
5%
 2,
 42.0
 et al. (2010a).

$\delta^{18}\text{O} = 0.0020052$,
 $\delta^{18}\text{O} = 5.31\%$ (et al.
 2010b).

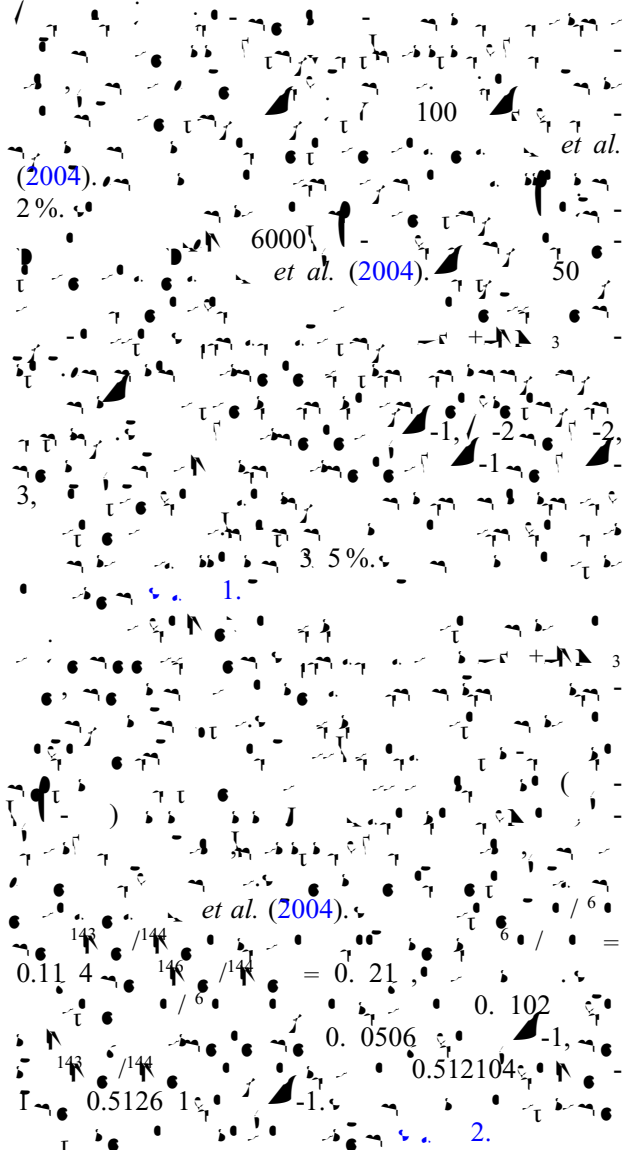
$\delta^{18}\text{O} = 5.44 \pm 0.21\%$ (2),
 $\delta^{18}\text{O} = 5.4 \pm 0.2\%$ (et al. 2013).

3.b. M a a a a

00
 15
 15

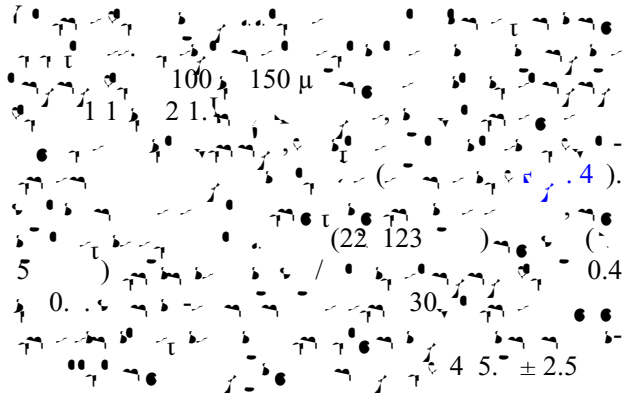


3.c. W a a a a



4. A a t e a l t

4.a. Z e c U Pb a



	2013 01-1	2013 01-3	2013 01-4	2013 01-5	2013 01-6	2013 01-	2013 01-	2013 01-1	2013 01-2	2013 01-4
<i>Major elements (%)</i>										
SiO ₂	3.0	4.20	3.41	3.62	3.22	3.2	3.05	4.22	46.4	51.2
TiO ₂	0.05	0.20	0.05	0.05	0.04	0.05	0.04	0.14	0.12	0.2
Al ₂ O ₃	0.61	1.6	1.04	0.6	0.0	0.4	0.0	1.2	1.64	1.33
V	13.21(1.3.21)-5530 ⁴⁴ (1.4-5.11)	4.6	0.10	0.11	0.36	0.5	0.16	3.6	3.24	--6030.1(36)
MnO	3.21	24.5	3.2	3.0	0.11	0.11	0.0	0.11	0.0	0.0
K ₂ O	0.12	15.42	0.15	0.14	0.2	0.10	0.142	0(0.11)-(0.0)	10.5. - .1431	42.5 5 4.3

Table 1.

	2013-01-1	2013-01-3	2013-01-4	2013-01-5	2013-01-6	2013-01-	2013-01-	2013-01-1	2013-01-2	2013-01-4
	2013-01-5	2013-01-6	2013-01- (\$\text{€}^{-1}\$)	2013-01- (\$\text{€}^{-1}\$)	2013-01- (\$\text{€}^{-1}\$)	2013-03-2	2013-03-3	2013-03-4	2013-03-5	2013-01-3
<i>Major elements (%)</i>										
Si	4.1	45.	4 ..	53.1	51.1	50.40	50.54	50.52	51.22	52.3
Al	0.34	0.15	1.40	1.24	1.31	1.0	1.63	1.31	1.1	0.33
Mg	1.5	1.5	16.5	16.1	15.3	15.0	16.6	15.55	15.4	1.61
Ca	4.52	3.34	3.44
Na	0.0	0.0	0.11	0.10	0.11	0.13	0.11	0.14	0.12	0.0
K	6.	.42	4.0	4.2	4.41	5.	3.2	6.06	.14	4.
Sc	11.03	12.61	6.22	5.5	6.3	6.5	4.52	4.	.26	..0
Ti	4.6	.3	.2	.3	.00	4.52	.31	4.0	4.0	.11
V	0.13	0.11	0.3	0.31	0.42	2.04	0.33	1.2	2.03	0.1
Cr	0.04	0.02	0.62	0.62	0.65	0.4	0.6	0.4	0.44	0.04
Mn	3.2	3.26	4.24	2.54	2.3	2.2	5.14	2.65	1.3	2.
Fe	..5	..2	..6	..0	..4	..40	..1	..6	..6	..1
Co	..4	..4	..11	..0	..42	..56	..64	..6	..11	..2
Ni	5	1	55	54	54	56	41	56	64	4
<i>Trace elements (ppm)</i>										
As	0	4.5	1.16	1.12	1.4	0	40.4	5.2	6.2	5.1
Se	0.22	0.135	1.24	1.63	1.316	1.53	1.034	1.100	0.55	0.62
Br	25.0	23.	1.6	1.5	1.5	1.5	1.2	25.2	1.	1.0
Cl	11	3.	1.6	166	1.2	22	22	254	1.	5.
S	34.	163	60.5	62.6	64.1	116	1.	0.	203	23.
P	24.2	21.6	26.	23.6	24.6	2.	2.5	2.0	2.0	16.4
SiO ₂	4.	1.5	63.6	50.	51.4	6.	2.	5.3	132	1.1

	2013 01-5	2013 01-6	2013 01-7	2013 01-8	2013 01-9	2013 03-2	2013 03-3	2013 03-4	2013 03-5	2013 01-3	
23.40	3.	1.20	(1)	(1)	46.0	4 .30	23.40	43.00	25.20	32.0	(1)

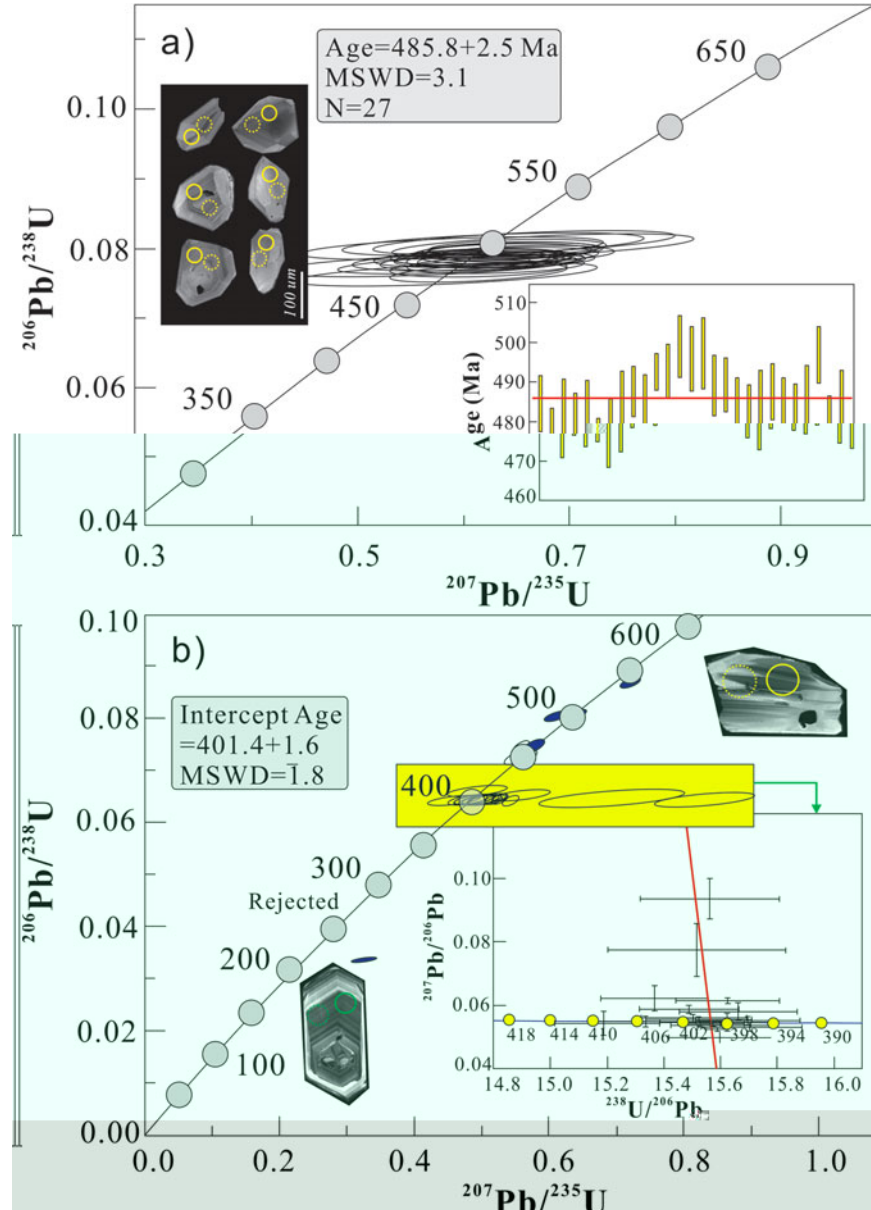
Table 1.

	2013-01-11 (\pm 2)	2013-02-1 (\pm 2)	2013-02-2 (\pm 2)	2013-03-1 (\pm 1)	2013-03-6 (\pm 1)	2013-01-10 (\pm 2)	04-06 (\pm 1)	04-24 (\pm 1)	04-2 (\pm 1)	03-1 (\pm 1)
Trace elements (ppm)										
Al	1.4	36.	42.4	26.0	32.4	1.	/	/	/	/
Ca	0.35	0.153	0.35	1.1	0.4	0.46	/	/	/	/
Cr	32.5	33.2	34.5	25.1	26.3	32.1	13.4	20.5	1.	20.3
Fe	1.4	203	21	33	341	1.5	144	14	214	265
Mn	56.5	44.2	4.	1.	22.2	53.	15	162	214	265
Ni	34.	3.5	3.3	23.1	24.	33.	20.6	30.	2.	20.2
Pb	66.4	4.6	6.4	25.4	2.1	66.6	1.	114	5.5	.02
Si	6.4	236.4	256.	205.4	20	114.20	/	/	/	/
Ti	4.0	44.1	4.0	4.	103	44.1	/	/	/	/
V	12.0	11.1	11.2	14.	13.6	12.0	/	/	/	/
Zn	0.5	1.420	1.00	3.130	3.20	0.53	4.	1.1	22.0	1.2
As	1	1.50	5	20	24	66	1	31	111	6
Br	13.0	13.0	13.2	21.1	22.	12.5	13.2	13.2	14.	20.1
Cu	54.	42.3	41.5	144	154	52.	243	133	164	151
Li	1.2	0.4	0.55	11.315	11.5	1.25	20.2	12.	21.	12.2
Na	0.025	0.030	0.02	0.051	0.052	0.02	/	/	/	/
K	0.31	0.26	0.32	1.560	1.450	0.360	/	/	/	/
Rb	0.2	1.20	1.030	0.365	0.406	0.336	/	/	/	/
Y	11	32	346	25	50	4.3	/	/	/	/
Sc	10.0	.40	.610	26.40	26.0	10.50	30.6	32.2	40.1	26.4
Th	23.00	1.0	1.40	51.50	54.0	22.30	5.	62.	2.3	52.5
Hf	2.0	2.520	2.510	5.50	6.10	2.60	6.	4	10.5	6.4
Ta	11.0	11.0	11.60	22.30	24.30	11.60	2.5	31.2	43.1	24.4
W	2.540	2.00	2.60	4.40	4.00	2.30	4.5	5.2	6.	4.5
Os	0.6	0.1	0.0	1.163	1.25	0.3	1.45	1.5	2.0	1.03
Ir	2.40	2.13	2.54	4.14	4.46	2.522	3.56	4.01	5.35	4.23
Pt	0.36	0.3	0.3	0.612	0.660	0.34	0.4	0.54	0.64	0.63
Pd	2.10	2.150	2.220	3.420	3.60	2.130	2.5	2.	3.24	3.5
Ag	0.46	0.446	0.444	0.2	0.5	0.46	0.4	0.52	0.5	0.
As	1.350	1.230	1.240	2.120	2.20	1.310	1.32	1.3	1.45	2.25
Se	0.10	0.16	0.15	0.304	0.32	0.14	0.1	0.2	0.2	0.34
Te	1.210	1.050	1.120	1.60	2.110	1.210	1.25	1.23	1.24	2.13
Sn	0.14	0.164	0.165	0.21	0.323	0.13	0.20	0.1	0.1	0.34
Sb	1.30	0.41	1.040	3.20	3.510	1.460	5.3	3.2	4.16	3.2
Bi	0.04	0.062	0.051	0.5	0.644	0.0	1.35	0.6	1.16	0.6
As	0.151	2.0	1.50	2.5	1.	0.33	/	/	/	/
Se	0.34	0.206	0.200	45.20	35.10	0.41	.13	.0	4.1	21.06
Te	1.0	0.61	0.1	.60	.20	1.0	4.50	2.63	3.20	.41
Sn	0.500	0.304	0.302	2.30	3.40	0.501	1.	0.6	1.46	.25

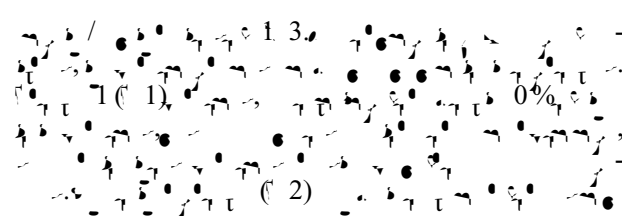
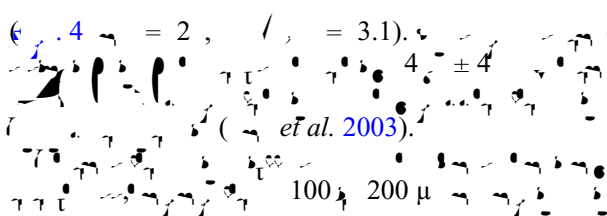
04-06, 04-26, 04-2, 04-1, et al. (2009a).

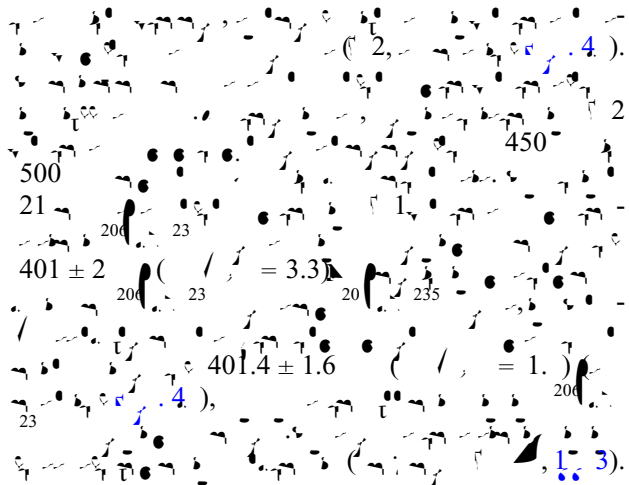
	U_{tot}	U_{REE}	$\text{U}_{\text{REE}} / \text{U}_{\text{tot}}$	$\text{U}_{\text{REE}} / \text{U}_{\text{tot}} (1\sigma)$	$\text{U}_{\text{REE}} / \text{U}_{\text{tot}}$	$\text{U}_{\text{REE}} / \text{U}_{\text{tot}} (1\sigma)$	$\text{U}_{\text{REE}} / \text{U}_{\text{tot}}$	$\text{U}_{\text{REE}} / \text{U}_{\text{tot}} (1\sigma)$	$\text{U}_{\text{REE}} / \text{U}_{\text{tot}}$	$\text{U}_{\text{REE}} / \text{U}_{\text{tot}} (1\sigma)$	
2013-01-3	0.36	3.2	0.002	0.04030(2)	0.04015	2.4	10.	0.13	4	0.5123(40)	0.512446
2013-01-10	0.5	6.6	0.0024	0.045(23)	0.0445	2.3	11.6	0.1235	0.5120(43)	0.512461	
2013-03-1	3.13	2.0	0.0335	0.06324(20)	0.06133	4.4	22.3	0.121	0.512533(4)	0.5122141	
2013-03-2	2.	1320	0.0063	0.042(20)	0.04255	4.5	2.6	0.1046	0.5121(51)	0.5124456.3	
2013-03-3	.06	516	0.0452	0.0536(43)	0.05111	5.	36.	0.0	0.5120(30)	0.5124506.4	
2013-03-4	.65	14.0	0.01	0.0422(51)	0.04120	4.55	24.5	0.1123	0.51203(53)	0.51250.5	

$$\text{f}(t) = 10000((^{143}\text{La} / ^{144}\text{La}) (t) / (^{143}\text{La} / ^{144}\text{La})_0 - 1) \text{f}(t) + (10 / 60) \quad t > 0 \quad t < 0$$



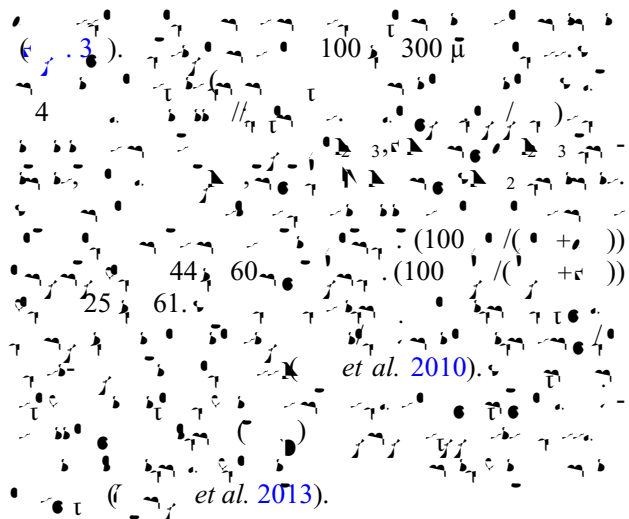
4. $\text{U}_{\text{REE}} / \text{U}_{\text{tot}} = 2$, $\text{U}_{\text{REE}} / \text{U}_{\text{tot}} = 3.1$, $\text{U}_{\text{REE}} / \text{U}_{\text{tot}} = 4 \pm 4$ (*Wang et al. 2003*).



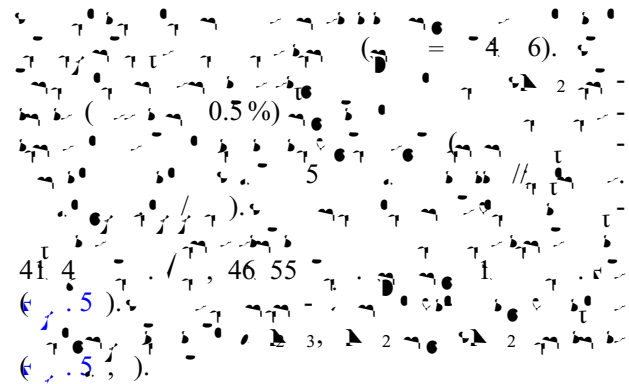


4.b. Mineral compositions

4.b.1. Spinel composition



4.b.2. Pyroxene compositions



4.c. Whole-rock trace elements

4.c.1. Serpentinites and cumulates

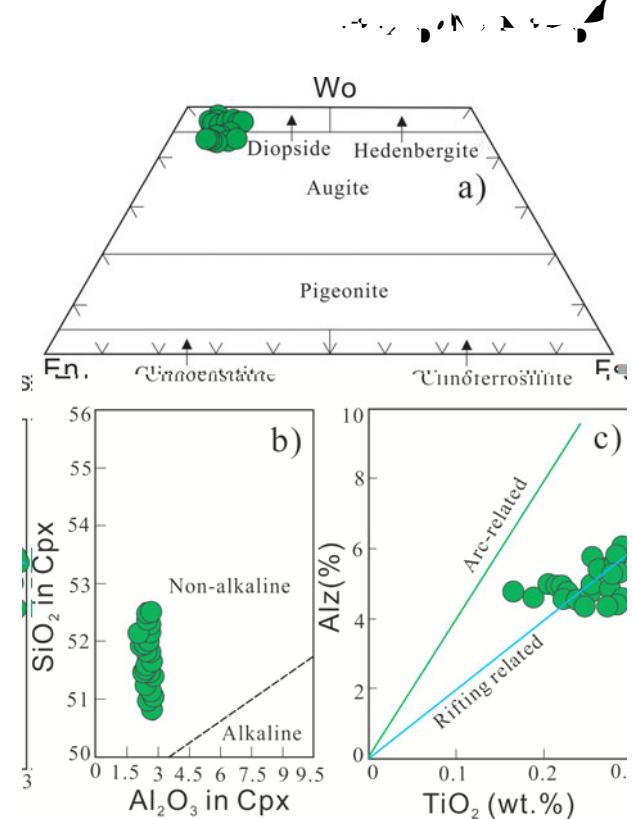
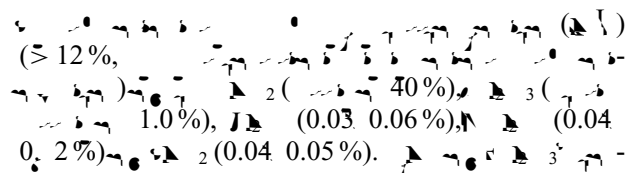
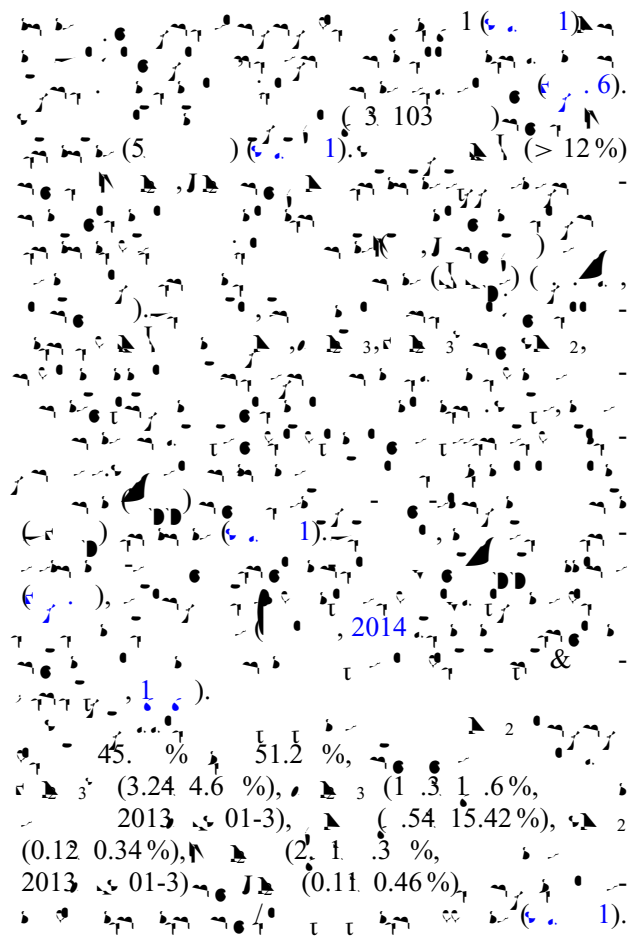


Fig. 4. Mineralogical and geochemical data for the study area. (a) Wo-Er-Fr triangular plot showing mineral stability fields for Diopside, Hedenbergite, Augite, and Pigeonite. (b) SiO_2 in Cpx vs Al_2O_3 in Cpx diagram. (c) $\text{Alz}(\%)$ vs TiO_2 (wt.%) diagram showing arc-related and rifting-related trends.



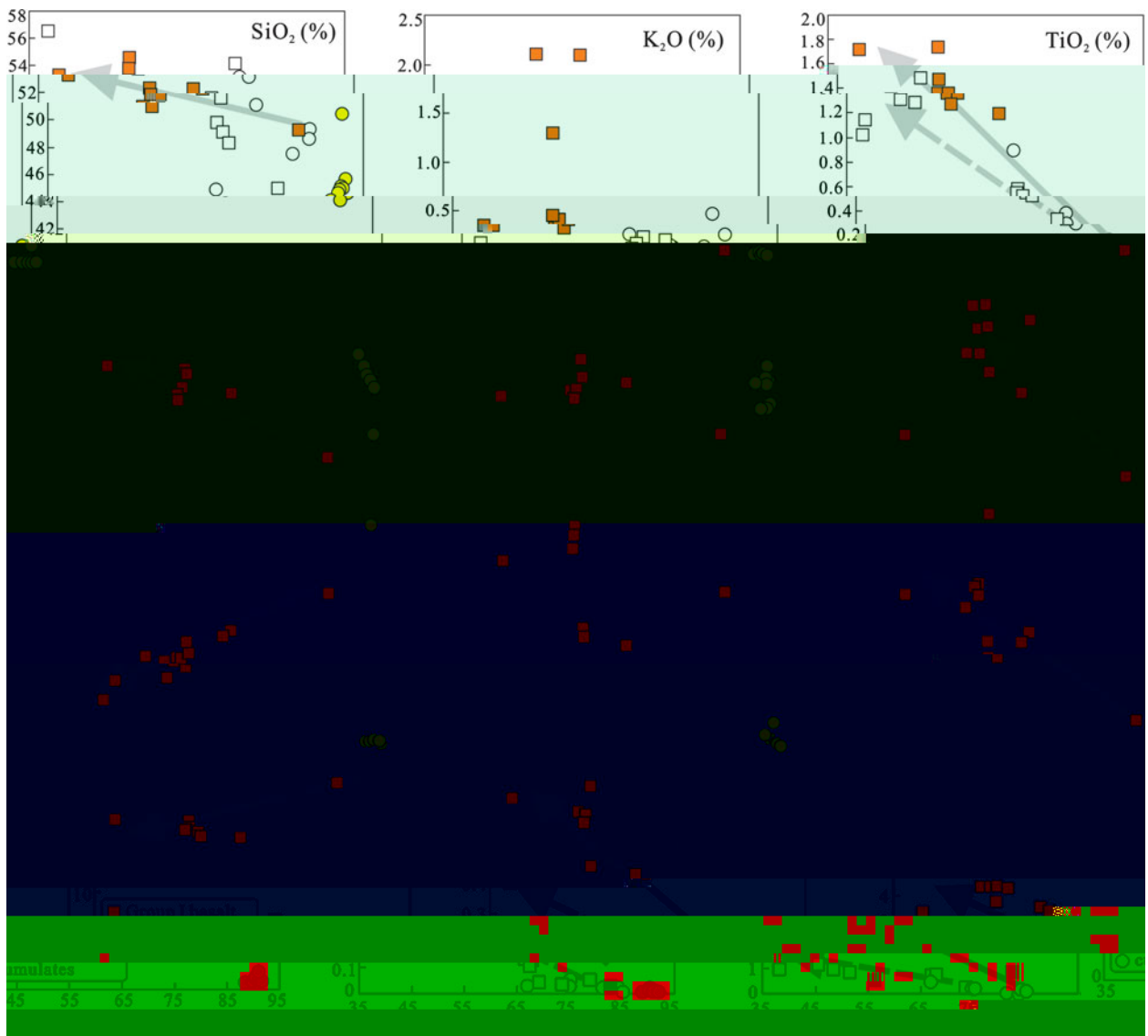
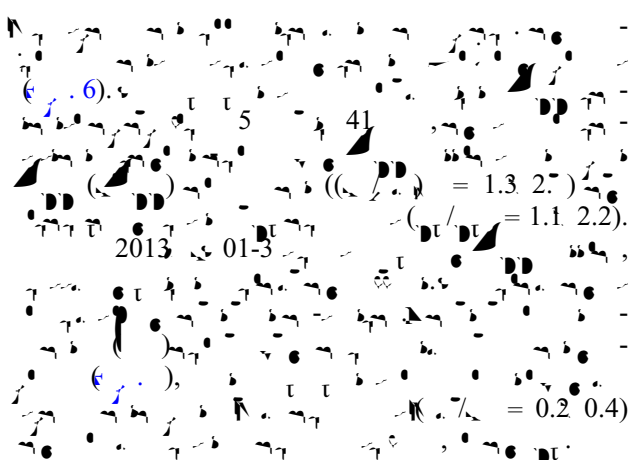
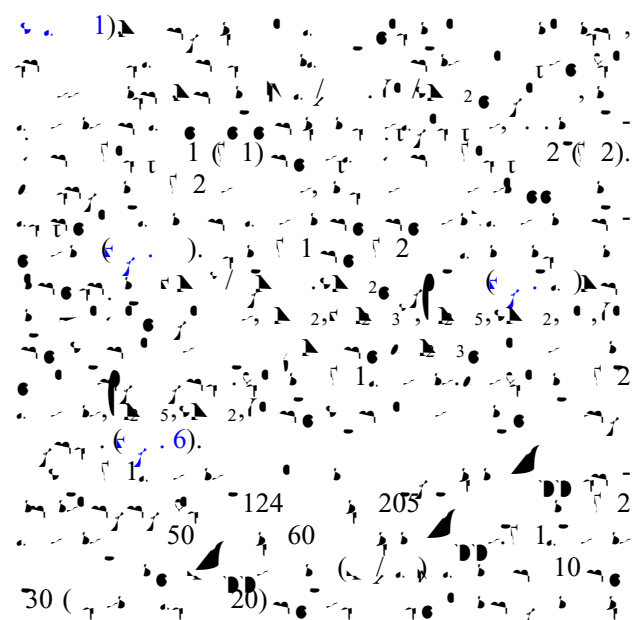


Fig. 6. (a) Variation of major elements (wt%) versus Mg# for the Zhaheba ophiolite (this study) and other ophiolites (modified after Li et al. 2009; Chen et al. 2009; Liu et al. 2009; Wang et al. 2009).



4.c.2. Basalts

The basalts have a range of compositions from 43.15% to 55.65% (Mg# = 42–52%,



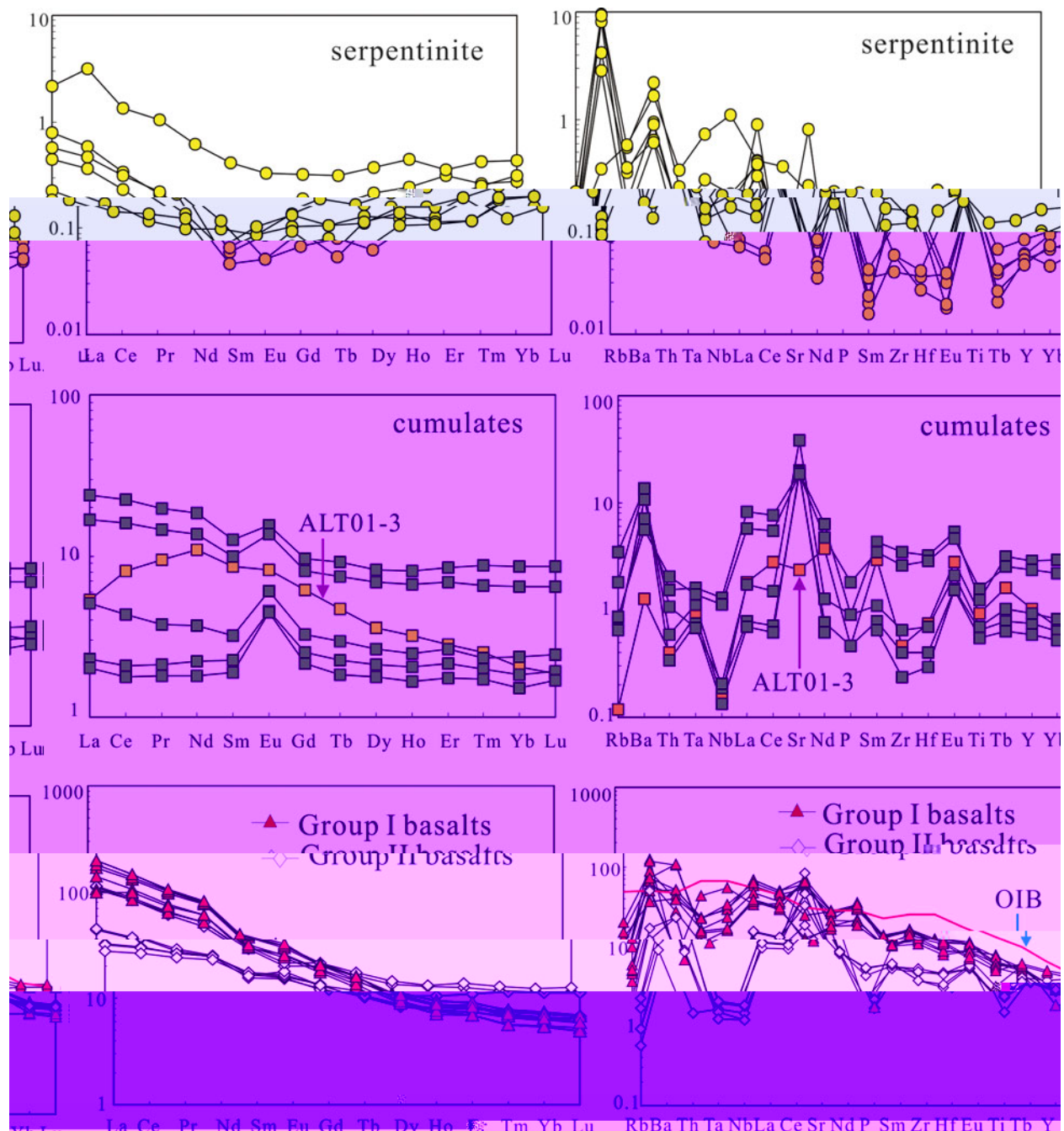


Fig. 1. Trace element patterns of the serpentinite, cumulates and basalts. The patterns are plotted against the ratios of incompatible elements (e.g., Lu/Yb, La/Sm, etc.) to correct for the effects of varying degrees of partial melting and differentiation. The patterns are plotted on a log-linear scale. The patterns for the serpentinite and cumulates are relatively simple, showing a general decrease in element concentration with increasing element size. The patterns for the basalts are more complex, showing a variety of trends, including positive and negative anomalies, and some degree of fractionation.

Fig. 2. Trace element patterns of the serpentinite, cumulates and basalts. The patterns are plotted against the ratios of incompatible elements (e.g., Lu/Yb, La/Sm, etc.) to correct for the effects of varying degrees of partial melting and differentiation. The patterns are plotted on a log-linear scale. The patterns for the serpentinite and cumulates are relatively simple, showing a general decrease in element concentration with increasing element size. The patterns for the basalts are more complex, showing a variety of trends, including positive and negative anomalies, and some degree of fractionation.

Fig. 3. Whole-rock Sr, Nd, Sr, Hf, O, and Y patterns of the serpentinite, cumulates and basalts. The patterns are plotted against the ratios of incompatible elements (e.g., Lu/Yb, La/Sm, etc.) to correct for the effects of varying degrees of partial melting and differentiation. The patterns are plotted on a log-linear scale. The patterns for the serpentinite and cumulates are relatively simple, showing a general decrease in element concentration with increasing element size. The patterns for the basalts are more complex, showing a variety of trends, including positive and negative anomalies, and some degree of fractionation.

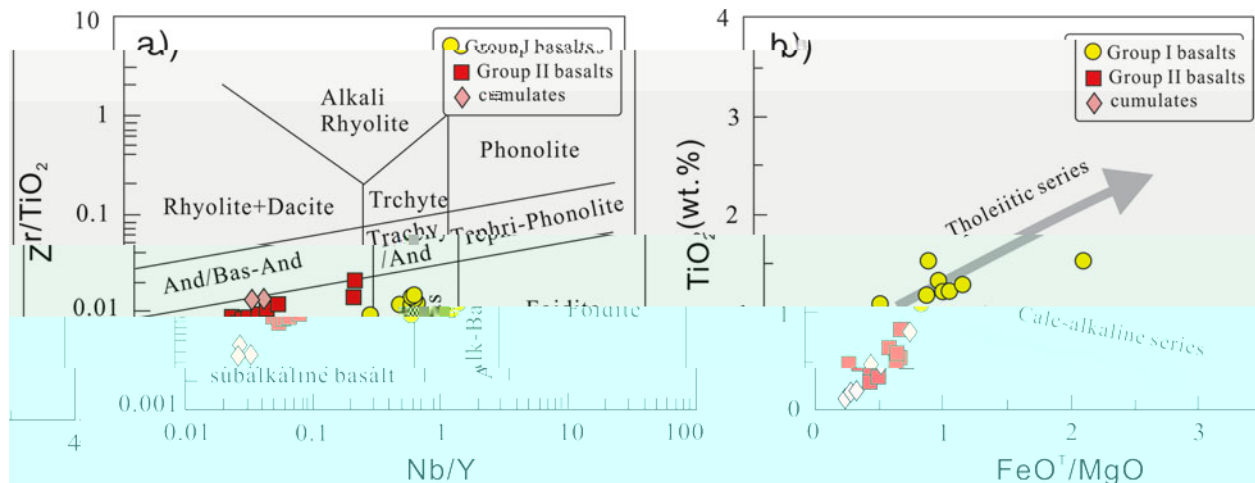


Fig. 5. (a) Zr/TiO₂ vs. Nb/Y and (b) TiO₂ (wt. %) vs. FeO²/MgO. The shaded area at the bottom left of plot (a) represents subalkaline basalt (Le Maitre et al., 1989).

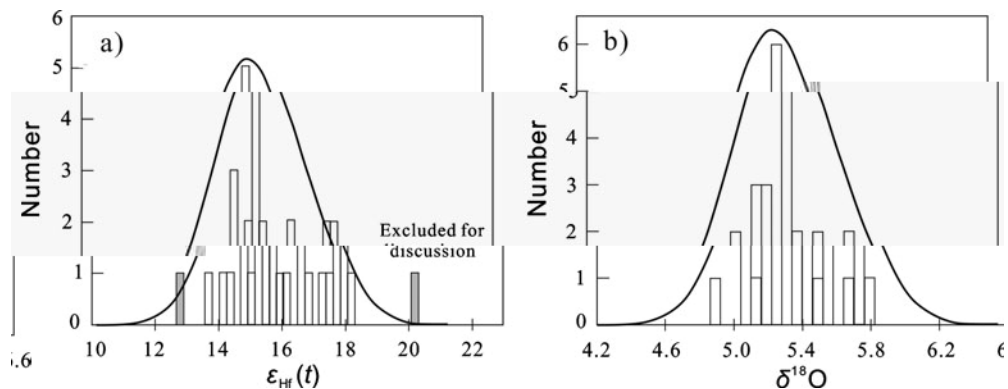


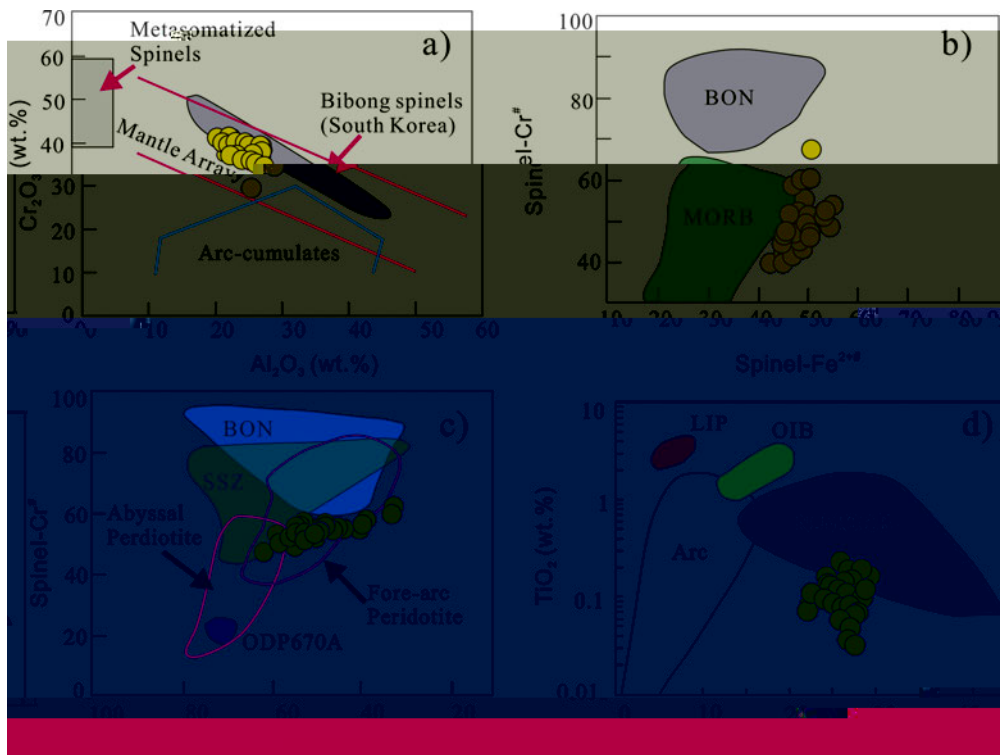
Fig. 6. Histograms of ε_{Hf}(t) and δ¹⁸O values.

Fig. 6. Histograms of ε_{Hf}(t) and δ¹⁸O values. The shaded area at the bottom left of plot (a) represents subalkaline basalt (Le Maitre et al., 1989). The shaded area at the bottom left of plot (b) represents the excluded samples (ε_{Hf}(t) > 16 and δ¹⁸O < 4.5). The peak of ε_{Hf}(t) is at ~15.5, and the peak of δ¹⁸O is at ~5.4. The number of samples is ~400. The ε_{Hf}(t) and δ¹⁸O values are plotted in Fig. 7.

5. Discussion

5.a. Tectonic setting

The tectonic setting of the Zhaheba ophiolite is discussed based on the geological features and geochemical characteristics. The ophiolite is situated in the northern margin of the South China Sea, where the South China Sea plate subducts beneath the continental crust. The ophiolite exhibits typical features of an island arc ophiolite, such as high-pressure metamorphism, ultramylonite zones, and eclogite facies rocks. The presence of amphibolites and granulites indicates high-pressure conditions during the formation of the ophiolite. The geochemical characteristics of the basalts and cumulates also support this interpretation. The basalts show enrichment in incompatible elements (e.g., Ti, Zr, Hf, Y, La, Ce, Nd, Eu, Sr, Ba, Pb, U, Th, and Pb) and depletion in compatible elements (e.g., Ti, Zr, Hf, Y, La, Ce, Nd, Eu, Sr, Ba, Pb, U, Th, and Pb). This pattern is typical of island arc magmatism, where the basalts are derived from the melting of subducting oceanic crust or mantle wedge. The presence of cumulates suggests that the melt was partially differentiated before reaching the surface. The high TiO₂ and FeO²/MgO values indicate a tholeiitic differentiation trend, while the low TiO₂ and high FeO²/MgO values indicate a calc-alkaline differentiation trend. The ε_{Hf}(t) values range from -10 to +10, and the δ¹⁸O values range from 4.5 to 5.5. These values are typical for island arc magmatism, where the basalts are derived from the melting of subducting oceanic crust or mantle wedge.

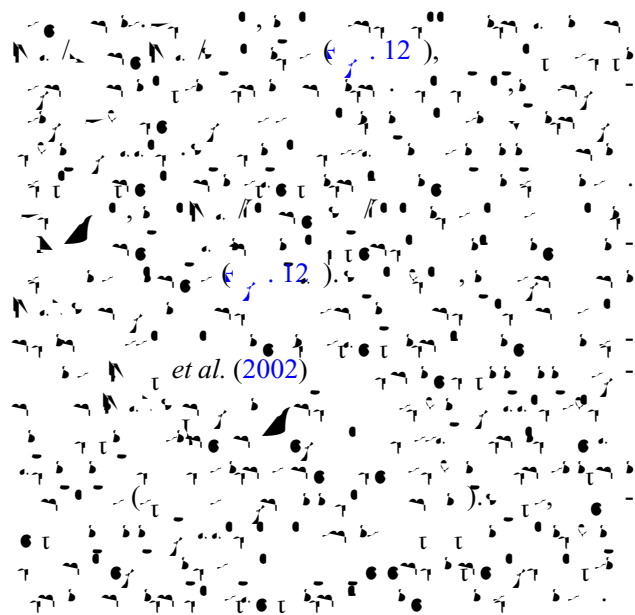
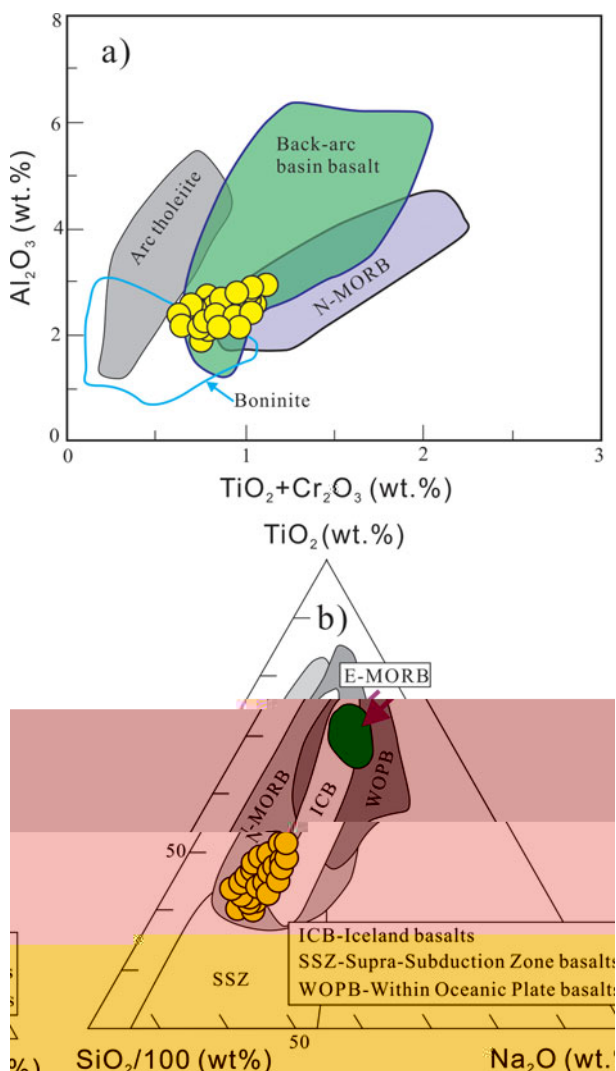


& ¹⁰, 2000), $(100 \text{ Cr}^{2+}/(\text{Cr}^{2+} + \text{Al}^{3+}))$ & ¹¹, 2001), $(100 \text{ Cr}^{2+}/(\text{Cr}^{2+} + \text{Al}^{3+}))$ & ¹², 2001), $(100 \text{ Cr}^{2+}/(\text{Cr}^{2+} + \text{Al}^{3+}))$ & ¹³, 2001), $(100 \text{ Cr}^{2+}/(\text{Cr}^{2+} + \text{Al}^{3+}))$ & ¹⁴, 2001). $\text{Cr}/(\text{Cr} + \text{Al})$ & ¹⁵, 2001). $\text{Cr}/(\text{Cr} + \text{Al})$ & ¹⁶, 2001). $\text{Cr}/(\text{Cr} + \text{Al})$ & ¹⁷, 2001). $\text{Cr}/(\text{Cr} + \text{Al})$ & ¹⁸, 2001). $\text{Cr}/(\text{Cr} + \text{Al})$ & ¹⁹, 2001). $\text{Cr}/(\text{Cr} + \text{Al})$ & ²⁰, 2001). $\text{Cr}/(\text{Cr} + \text{Al})$ & ²¹, 2001). $\text{Cr}/(\text{Cr} + \text{Al})$ & ²², 2001). $\text{Cr}/(\text{Cr} + \text{Al})$ & ²³, 2001). $\text{Cr}/(\text{Cr} + \text{Al})$ & ²⁴, 2001). $\text{Cr}/(\text{Cr} + \text{Al})$ & ²⁵, 2001). $\text{Cr}/(\text{Cr} + \text{Al})$ & ²⁶, 2001). $\text{Cr}/(\text{Cr} + \text{Al})$ & ²⁷, 2001). $\text{Cr}/(\text{Cr} + \text{Al})$ & ²⁸, 2001). $\text{Cr}/(\text{Cr} + \text{Al})$ & ²⁹, 2001). $\text{Cr}/(\text{Cr} + \text{Al})$ & ³⁰, 2001). $\text{Cr}/(\text{Cr} + \text{Al})$ & ³¹, 2001). $\text{Cr}/(\text{Cr} + \text{Al})$ & ³², 2001). $\text{Cr}/(\text{Cr} + \text{Al})$ & ³³, 2001). $\text{Cr}/(\text{Cr} + \text{Al})$ & ³⁴, 2001). $\text{Cr}/(\text{Cr} + \text{Al})$ & ³⁵, 2001). $\text{Cr}/(\text{Cr} + \text{Al})$ & ³⁶, 2001). $\text{Cr}/(\text{Cr} + \text{Al})$ & ³⁷, 2001). $\text{Cr}/(\text{Cr} + \text{Al})$ & ³⁸, 2001). $\text{Cr}/(\text{Cr} + \text{Al})$ & ³⁹, 2001). $\text{Cr}/(\text{Cr} + \text{Al})$ & ⁴⁰, 2001). $\text{Cr}/(\text{Cr} + \text{Al})$ & ⁴¹, 2001). $\text{Cr}/(\text{Cr} + \text{Al})$ & ⁴², 2001). $\text{Cr}/(\text{Cr} + \text{Al})$ & ⁴³, 2001). $\text{Cr}/(\text{Cr} + \text{Al})$ & ⁴⁴, 2001). $\text{Cr}/(\text{Cr} + \text{Al})$ & ⁴⁵, 2001). $\text{Cr}/(\text{Cr} + \text{Al})$ & ⁴⁶, 2001). $\text{Cr}/(\text{Cr} + \text{Al})$ & ⁴⁷, 2001). $\text{Cr}/(\text{Cr} + \text{Al})$ & ⁴⁸, 2001). $\text{Cr}/(\text{Cr} + \text{Al})$ & ⁴⁹, 2001). $\text{Cr}/(\text{Cr} + \text{Al})$ & ⁵⁰, 2001). $\text{Cr}/(\text{Cr} + \text{Al})$ & ⁵¹, 2001). $\text{Cr}/(\text{Cr} + \text{Al})$ & ⁵², 2001). $\text{Cr}/(\text{Cr} + \text{Al})$ & ⁵³, 2001). $\text{Cr}/(\text{Cr} + \text{Al})$ & ⁵⁴, 2001). $\text{Cr}/(\text{Cr} + \text{Al})$ & ⁵⁵, 2001). $\text{Cr}/(\text{Cr} + \text{Al})$ & ⁵⁶, 2001). $\text{Cr}/(\text{Cr} + \text{Al})$ & ⁵⁷, 2001). $\text{Cr}/(\text{Cr} + \text{Al})$ & ⁵⁸, 2001). $\text{Cr}/(\text{Cr} + \text{Al})$ & ⁵⁹, 2001). $\text{Cr}/(\text{Cr} + \text{Al})$ & ⁶⁰, 2001). $\text{Cr}/(\text{Cr} + \text{Al})$ & ⁶¹, 2001). $\text{Cr}/(\text{Cr} + \text{Al})$ & ⁶², 2001). $\text{Cr}/(\text{Cr} + \text{Al})$ & ⁶³, 2001). $\text{Cr}/(\text{Cr} + \text{Al})$ & ⁶⁴, 2001). $\text{Cr}/(\text{Cr} + \text{Al})$ & ⁶⁵, 2001). $\text{Cr}/(\text{Cr} + \text{Al})$ & ⁶⁶, 2001). $\text{Cr}/(\text{Cr} + \text{Al})$ & ⁶⁷, 2001). $\text{Cr}/(\text{Cr} + \text{Al})$ & ⁶⁸, 2001). $\text{Cr}/(\text{Cr} + \text{Al})$ & ⁶⁹, 2001). $\text{Cr}/(\text{Cr} + \text{Al})$ & ⁷⁰, 2001). $\text{Cr}/(\text{Cr} + \text{Al})$ & ⁷¹, 2001). $\text{Cr}/(\text{Cr} + \text{Al})$ & ⁷², 2001). $\text{Cr}/(\text{Cr} + \text{Al})$ & ⁷³, 2001). $\text{Cr}/(\text{Cr} + \text{Al})$ & ⁷⁴, 2001). $\text{Cr}/(\text{Cr} + \text{Al})$ & ⁷⁵, 2001). $\text{Cr}/(\text{Cr} + \text{Al})$ & ⁷⁶, 2001). $\text{Cr}/(\text{Cr} + \text{Al})$ & ⁷⁷, 2001). $\text{Cr}/(\text{Cr} + \text{Al})$ & ⁷⁸, 2001). $\text{Cr}/(\text{Cr} + \text{Al})$ & ⁷⁹, 2001). $\text{Cr}/(\text{Cr} + \text{Al})$ & ⁸⁰, 2001). $\text{Cr}/(\text{Cr} + \text{Al})$ & ⁸¹, 2001). $\text{Cr}/(\text{Cr} + \text{Al})$ & ⁸², 2001). $\text{Cr}/(\text{Cr} + \text{Al})$ & ⁸³, 2001). $\text{Cr}/(\text{Cr} + \text{Al})$ & ⁸⁴, 2001). $\text{Cr}/(\text{Cr} + \text{Al})$ & ⁸⁵, 2001). $\text{Cr}/(\text{Cr} + \text{Al})$ & ⁸⁶, 2001). $\text{Cr}/(\text{Cr} + \text{Al})$ & ⁸⁷, 2001). $\text{Cr}/(\text{Cr} + \text{Al})$ & ⁸⁸, 2001). $\text{Cr}/(\text{Cr} + \text{Al})$ & ⁸⁹, 2001). $\text{Cr}/(\text{Cr} + \text{Al})$ & ⁹⁰, 2001). $\text{Cr}/(\text{Cr} + \text{Al})$ & ⁹¹, 2001). $\text{Cr}/(\text{Cr} + \text{Al})$ & ⁹², 2001). $\text{Cr}/(\text{Cr} + \text{Al})$ & ⁹³, 2001). $\text{Cr}/(\text{Cr} + \text{Al})$ & ⁹⁴, 2001). $\text{Cr}/(\text{Cr} + \text{Al})$ & ⁹⁵, 2001). $\text{Cr}/(\text{Cr} + \text{Al})$ & ⁹⁶, 2001). $\text{Cr}/(\text{Cr} + \text{Al})$ & ⁹⁷, 2001). $\text{Cr}/(\text{Cr} + \text{Al})$ & ⁹⁸, 2001). $\text{Cr}/(\text{Cr} + \text{Al})$ & ⁹⁹, 2001). $\text{Cr}/(\text{Cr} + \text{Al})$ & ¹⁰⁰, 2001).

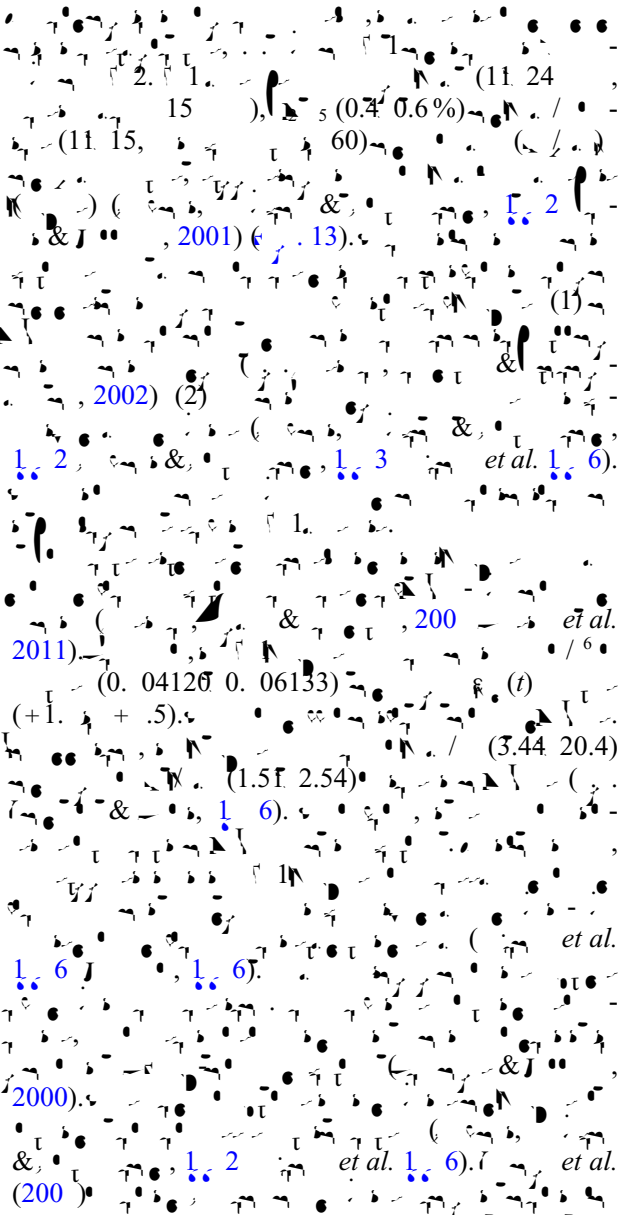
(500–400 °C) (*et al.* 2003; *et al.* 2015), (430–400 °C) (*et al.* 2003; *et al.* 2014), (300–350 °C) (*et al.* 2003; *et al.* 2006).

5.b. Olivine-rich melt accumulation

As discussed by *et al.* (2002) and *et al.* (2010),



5.c. Pt vs. D for the Zhaheba ophiolite



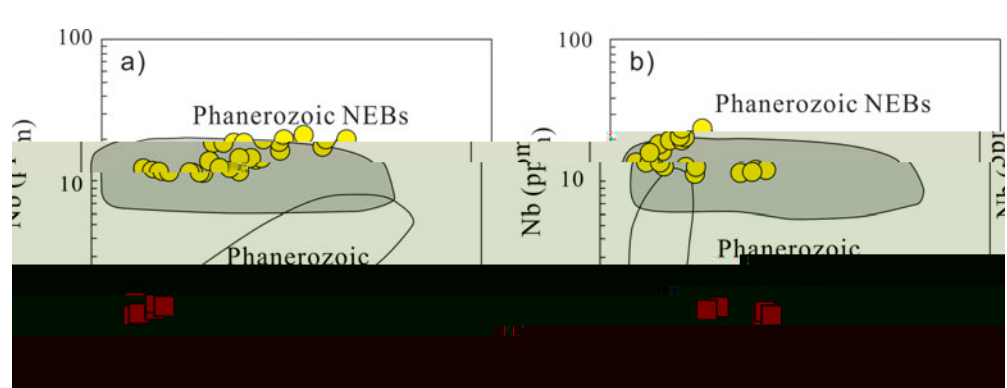
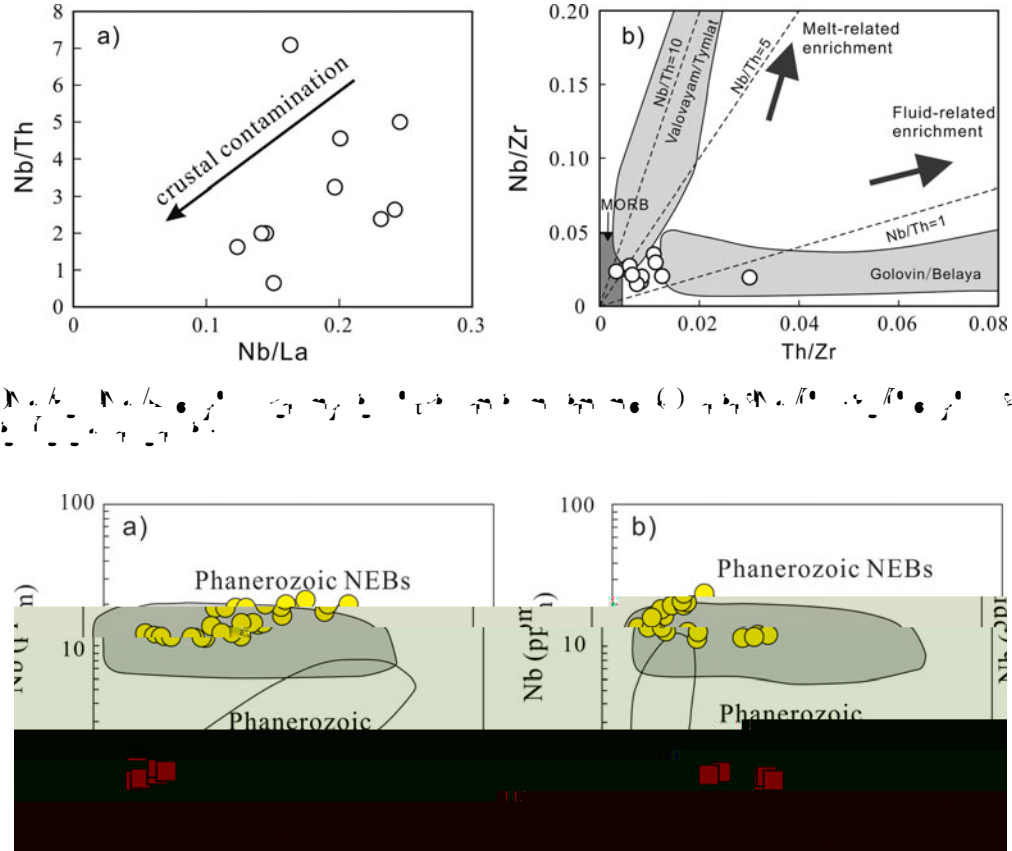


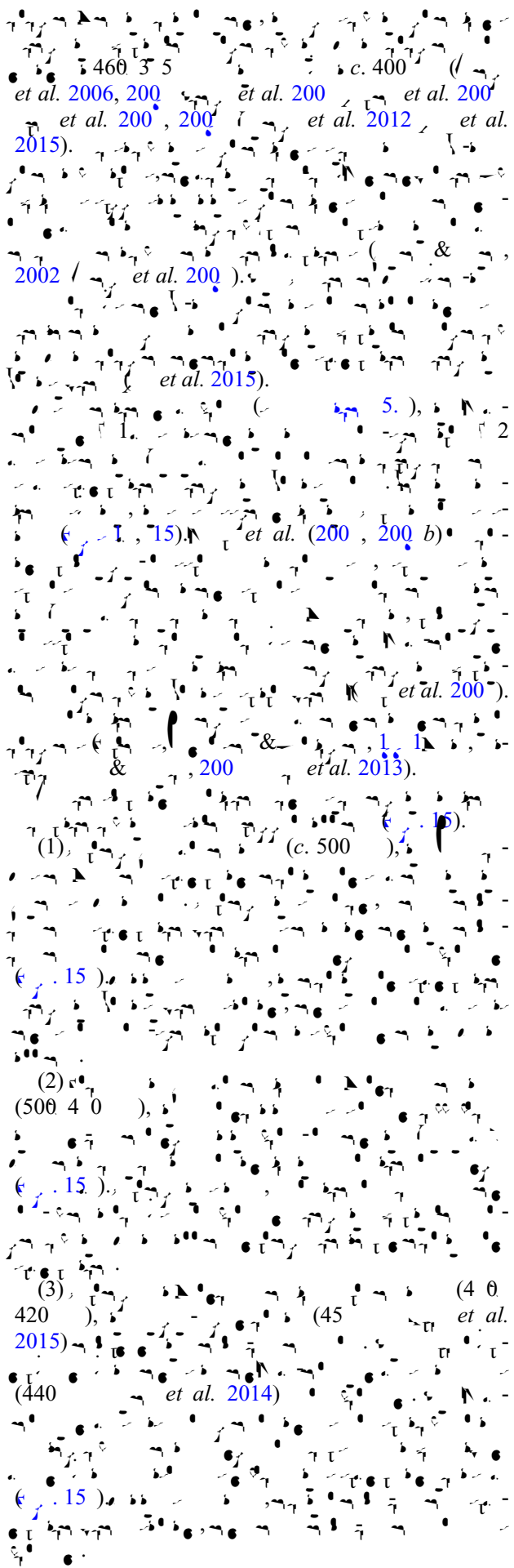
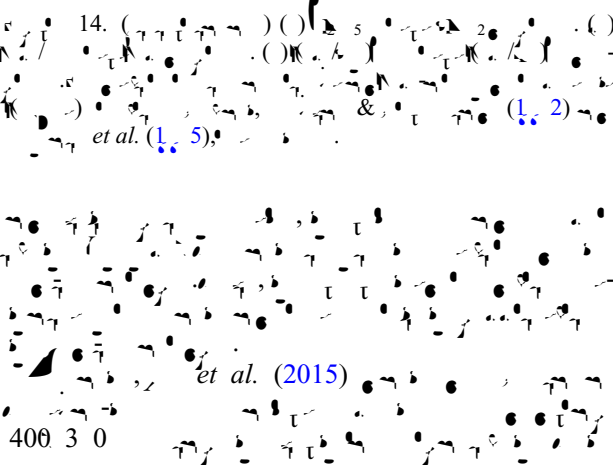
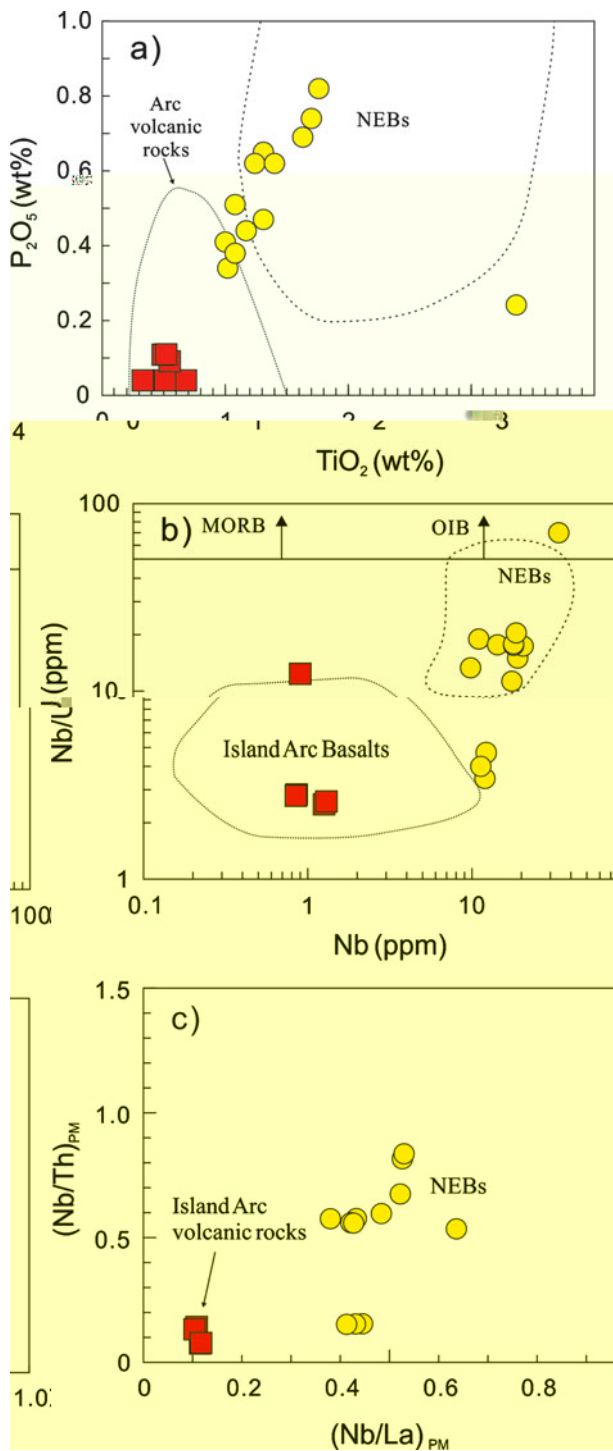
Fig. 12. The variation of Nb/Th vs. Nb/La (a) and Nb/Zr vs. Th/Zr (b). The linear trend in plot (a) is labeled 'crustal contamination'. The shaded field in plot (b) represents melt-related enrichment, and the field bounded by the dashed lines represents fluid-related enrichment. MORB and Golovin/Belyaia are also indicated.

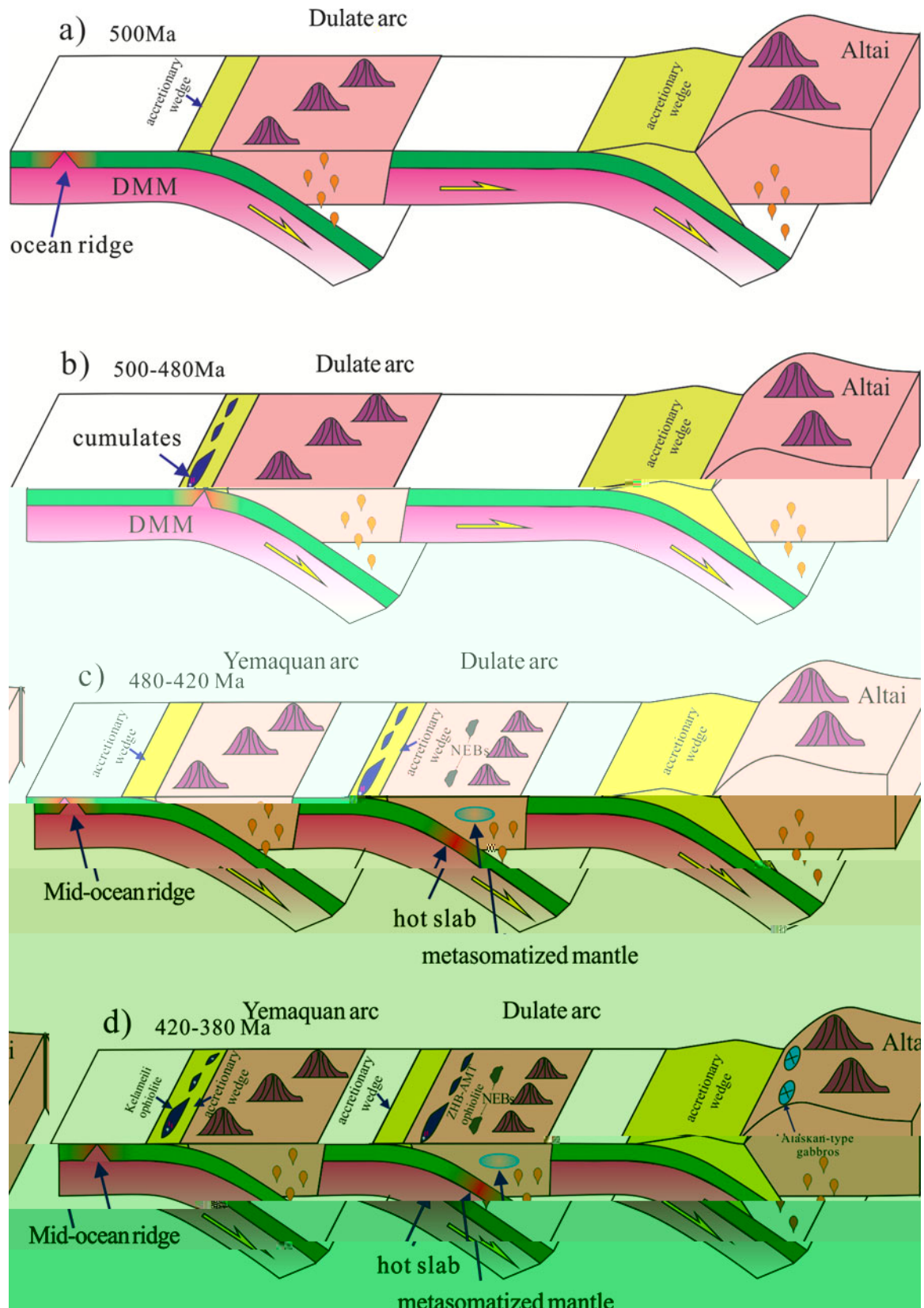
Fig. 13. Schematic representation of the Phanerozoic NEBs. The green layers represent the NEBs, and the red squares represent the host rocks. The scale bar indicates 100 μm .

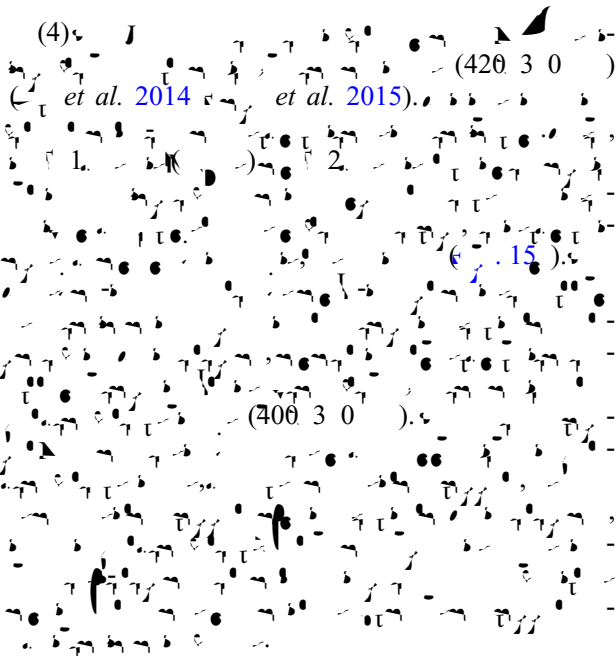
Fig. 14. The variation of Nb/Th vs. Nb/La (a) and Nb/Zr vs. Th/Zr (b) of the Phanerozoic NEBs. The values of Nb/Th and Nb/La are calculated based on the following ranges: < 0.3 , 0.3 – 0.5 , 0.5 – 1.0 , 1.0 – 2.0 , 2.0 – 3.0 , 3.0 – 4.0 , 4.0 – 5.0 , 5.0 – 6.0 , 6.0 – 7.0 , and > 7.0 . The values of Nb/Zr and Th/Zr are calculated based on the following ranges: 0.01 – 0.05 , 0.05 – 0.10 , 0.10 – 0.15 , 0.15 – 0.20 , 0.20 – 0.25 , 0.25 – 0.30 , 0.30 – 0.35 , 0.35 – 0.40 , 0.40 – 0.45 , and > 0.45 .

5.2. Identification of the Phanerozoic accretionary at Jia'an

Based on the geochemical characteristics of the Phanerozoic NEBs (Fig. 14), the NEBs at Jia'an were identified to be accreted to the continental margin of the South China Sea during the Paleogene (416–503 Ma) (Jia et al. 2014; Li et al. 2015), and the age of the NEBs is consistent with the ages of the NEBs in the Yanshan Orogen (496–503 Ma) (Liu et al. 2003; Li et al. 2015). The Phanerozoic NEBs are distributed along the continental margin of the South China Sea and in the South China Sea (Fig. 1). They are associated with the marginal basins of the South China Sea (400–500 m) (Fig. 1), and the thickness of the NEBs is approximately 100–200 m (Li et al. 2014). The Phanerozoic NEBs are primarily composed of shale, sandstone, and dolomite, and they are often interbedded with dolomitic limestone and dolomite.







6. Conclusion

- (1) The Zhaheba ophiolite has a wide range of compositions, from peridotites to gabbros. The Mg/(Mg+Fe) values range from ~0.45 to 1.0, and Cr/(Cr+Al) values range from ~0.15 to 1.0. The samples are divided into four groups based on their Mg/(Mg+Fe) and Cr/(Cr+Al) ratios.
 - (2) The Zhaheba ophiolite shows evidence of partial melting and differentiation. The presence of spinel inclusions in olivine suggests that the melt was partially molten. The presence of plagioclase inclusions in olivine suggests that the melt was partially molten.
 - (3) The Zhaheba ophiolite shows evidence of fractional crystallization. The presence of spinel inclusions in olivine suggests that the melt was partially molten. The presence of plagioclase inclusions in olivine suggests that the melt was partially molten.
- Accepted: 2016-03-01
Published online: 2016-06-03
DOI: 10.1017/et.2016.56
© 2016 Cambridge University Press
Printed in the United Kingdom

Supplementary data

<https://doi.org/10.1017/et.2016.56> 16000042.

References

- Akbari, M., & Ghosh, S. K. (2001). Petrogenesis of the ophiolitic rocks of the northern part of the Dharwar craton, South India. *Journal of Petrology*, *42*, 225–302.
- Baker, J. E., & Van Heege, J. (2000). The evolution of the Earth's crust and upper mantle. *Lithos*, *97*, 21–31.
- Baker, J. E., & Van Heege, J. (2002). The evolution of the Earth's crust and upper mantle. *Geology*, *30*, 10–11.
- Baker, J. E., & Van Heege, J. (2002). The evolution of the Earth's crust and upper mantle. *Earth Accretionary Systems in Space and Time* (Eds. J. E. Baker & J. Van Heege), p. 1–36. Geological Society of America Special Paper, 317.
- Baker, J. E., & Van Heege, J. (2002). The evolution of the Earth's crust and upper mantle. *Geological Magazine*, *139*, 1–13.
- Baker, J. E., & Van Heege, J. (2002). The evolution of the Earth's crust and upper mantle. *Geological Society of America Bulletin*, *105*, 15–31.
- Baker, J. E., & Van Heege, J. (2002). Ophiolites. *Geology*, *30*, 220–221.
- Baker, J. E., & Van Heege, J. (2002). The evolution of the Earth's crust and upper mantle. *Geology*, *21*, 54–56.
- Baker, J. E., & Van Heege, J. (2002). The evolution of the Earth's crust and upper mantle. *Journal of Geological Society, London*, *149*, 56–66.
- Baker, J. E., & Van Heege, J. (2003). The evolution of the Earth's crust and upper mantle. *Contributions to Mineralogy and Petrology*, *86*, 54–66.
- Baker, J. E., & Van Heege, J. (2003). The evolution of the Earth's crust and upper mantle. *Journal of Geological Society, London*, *160*, 21–31.
- Baker, J. E., & Van Heege, J. (2011). The evolution of the Earth's crust and upper mantle. *Geological Society of America Bulletin*, *123*, 37–411.
- Baker, J. E., & Van Heege, J. (2015). The evolution of the Earth's crust and upper mantle. *Chinese Journal of Geology*, *50*, 140–546.
- Baker, J. E., & Van Heege, J. (2000). The evolution of the Earth's crust and upper mantle. *Contributions to Mineralogy and Petrology*, *140*, 23–59.
- Baker, J. E., & Van Heege, J. (2000). The evolution of the Earth's crust and upper mantle. *Lithos*, *27*, 25–35.

- J., J., J., J., J., & J. 2011. *Geological Bulletin of China* 30, 150–153.
- J., J., J., J., & J. 2011. *Geochimica et Cosmochimica Acta* 75, 504–512.
- J., J., J., J., & J. 2001. *Nature* 410, 611.
- J., J., J., J., & J. 2002. *Chemical Geology* 182, 22–35.
- J., J., J., & J. 2006. *Journal of Geophysical Research: Solid Earth* (1978–2012) 101, 11–31.
- J., J., & J. 2000. *Contributions to Mineralogy and Petrology* 139, 20–26.
- J., J., J., J., J., J., & J. 2012. *Geological Bulletin of China* 31, 126.
- J., J., J., J., & J. 2014. *Chinese Science Bulletin (Chinese Version)* 59, 2213–2215.
- J., J., J., & J. 2000. *Transactions of the Royal Society of Edinburgh: Earth Sciences* 91, 1–3.
- J., J., J., & J. 2001. *Journal of Petrology* 31, 61–100.
- J., J., J., J., & J. 2003. *Earth Science Frontier* 10, 43–56.
- J., J., J., J., & J. 2001. *Journal of Petrology* 42, 655–665.
- J., J., J., J., & J. 2006. *Nature* 380, 23–40.
- J., J., J., J., & J. 2000. *Tectonophysics* 326, 255–265.
- J., J., J., J., & J. 2010a. *Geological Magazine* 141, 225–31.
- J., J., J., J., & J. 2010b. *Geostandards and Geoanalytical Research* 34, 11–34.
- J., J., J., J., & J. 2013. *Chinese Science Bulletin* 58, 464–474.
- J., J., & J. 2000. *Lithos* 113, 24–31.
- J., J., J., & J. 2010. *Chinese Science Bulletin* 55, 1535–1546.
- J. 2003. *User's Manual for Isoplot 3.00: A Geochronological Toolkit for Microsoft Excel*.
- J., J., J., J., & J. 2015. *Gondwana Research*, 10.1016/j.gr.2015.04.004.
- J., J., J., J., & J. 2015. *American Journal of Science* 274, 32–355.
- J., J., J., J., & J. 2015. *Geology* 43, 51–54.
- J., J., J., J., & J. 2015. *Structure of Ophiolites and Dynamics of Oceanic Lithosphere*.
- J., J., J., J., & J. 2015. *Journal of Petrology* 56, 104–124.
- J., J., J., J., & J. 2000. *Acta Petrologica Sinica* 16, 247–256.
- J., J., J., J., & J. 2000. *Acta Petrologica Sinica* 14, 4, 1–16.
- J., J., J., J., & J. 2000. *Acta Petrologica Sinica* 23, 162–174.
- J., J., J., J., & J. 2002. *Acta Petrologica Sinica* 16, 1–16.
- J., J., J., J., & J. 2002. *Proceedings of the Ocean Drilling Program, Scientific Results*, vol. 176(1–1), 1–60.

- W., & . 200 .
Chinese Science Bulletin 14, 21 6 71.
- W., & . 2010.
Lithos 117, 1 20 .
- W., & . 200 .
Journal of Asian Earth Sciences 30, 666 5 .
- W., . 200 .
Lithos 100, 14 4 .
- W., 2014.
Elements 10, 101 .
- W., & . 2001.
Contribution to Mineralogy and Petrology 141, 36 52.
- W., & . 2013.
Gondwana Research 24, 3 2 411.
- W., & . 200 .
Journal of Petrology 37, 6 3 26.
- W., & . 2013.
Precambrian Research 231, 301 24.
- W., & . 2012.
Precambrian Research 192 195, 1 0 20 .
- W., & . 200 .
Philosophical Transactions of the Royal Society of London 335, 3 2 .
- W., & . 2014. (~440) .
Nature 377, 5 5 600.
- W., & . 200 .
Nature 364, 2 30 .
- W., & . 2014. (~440) .
Lithos 206 207, 234 51.
- W., 2002. .
Reviews of Geophysics 40, 3-1 3-3 .
- W., & . 200 .
Chemical Geology 247, 352 3 .
- W., & . 200 .
Acta Petrologica Sinica 23, 1 33 44 .
- W., & . 200 .
Contributions to Mineralogy and Petrology 133, 1 11.
- W., & . 2006.
Journal of Geology 114, 35 51.
- W., & . 200 .
Lithos 110, 35 2 .
- W., & . 2012.
Earth-Science Reviews 113, 303 41.
- W., & . 200 .
Chemical Geology 20, 325 43.
- W., & . 2002.
Journal of Geology 110, 1 3 .
- W., & . 2006.
Geology in China 33, 4 6 66 .
- W., & . 2014.
Geoscience Frontiers 5, 525 36.
- W., & . 200 .
Journal of Asian Earth Sciences 32, 102 1 .
- W., & . 2013.
Gondwana Research 23, 1316 41.
- W., & . 2004.
Journal of Geological Society, London 161, 33 42.
- W., & . 200 .
Science in China Series D - Earth Sciences 52, 1345 5 .
- W., & . 200 .
Magmatism in the Ocean Basin (. & .), 52, 4 42 .
- W., & . 200 .
Chemical Geology 247, 352 3 .
- W., & . 200 .
Acta Petrologica Sinica 23, 1 33 44 .
- W., & . 200 .
Contributions to Mineralogy and Petrology 133, 1 11.
- W., & . 2006.
Journal of Geology 114, 35 51.
- W., & . 200 .
Lithos 110, 35 2 .
- W., & . 2012.
Earth-Science Reviews 113, 303 41.
- W., & . 200 .
Chemical Geology 20, 325 43.
- W., & . 2002.
Journal of Geology 110, 1 3 .
- W., & . 2006.
Geology in China 33, 4 6 66 .
- W., & . 2014.
Geoscience Frontiers 5, 525 36.
- W., & . 200 .
Journal of Asian Earth Sciences 32, 102 1 .
- W., & . 2013.
Gondwana Research 23, 1316 41.
- W., & . 2004.
Journal of Geological Society, London 161, 33 42.

- Wang, L., Li, Y., & Li, J. 2000. *a.* Regional geological setting and magmatic evolution of the Zhaheba ophiolite, South Tianshan, China. *International Journal of Earth Sciences* **98**, 11–21.
- Wang, L., Li, Y., & Li, J. 2000. *b.* Magmatic evolution of the Zhaheba ophiolite, South Tianshan, China. *American Journal of Sciences* **309**, 221–240.
- Wang, L., Li, Y., & Li, J. 2003. Regional Geology of the Xinjiang Uygur Autonomous Region. *Geological Survey of China*, 2, 145 (in Chinese).
- Wang, L., Li, Y., & Li, J. 2015. Magmatic evolution of the Zhaheba ophiolite, South Tianshan, China. *Journal of Asian Earth Sciences* **113**, 5–15.
- Wang, L., Li, Y., & Li, J. 2012. Magmatic evolution of the Zhaheba ophiolite, South Tianshan, China. *Gondwana Research* **21**, 246–265.
- Wang, L., Li, Y., & Li, J. 2000. *c.* Magmatic evolution of the Zhaheba ophiolite, South Tianshan, China. *Chemical Geology* **242**, 223–240.
- Wang, L., Li, Y., & Li, J. 2006. Magmatic evolution of the Zhaheba ophiolite, South Tianshan, China. *Acta Geologica Sinica* **80**, 254–263.
- Wang, L., Li, Y., & Li, J. 2003. Magmatic evolution of the Zhaheba ophiolite, South Tianshan, China. *Chinese Science Bulletin* **48**, 2231–2235.
- Wang, L., Li, Y., & Li, J. 2013. Magmatic evolution of the Zhaheba ophiolite, South Tianshan, China. *Lithos* **179**, 263–274.
- Wang, L., Li, Y., & Li, J. 2012. Magmatic evolution of the Zhaheba ophiolite, South Tianshan, China. *Journal of Asian Earth Sciences* **52**, 11–33.
- Wang, L., Li, Y., & Li, J. 2000. *d.* Magmatic evolution of the Zhaheba ophiolite, South Tianshan, China. *Acta Petrologica Sinica* **24**, 1054–1063.
- Wang, L., Li, Y., & Li, J. 2001. *e.* Magmatic evolution of the Zhaheba ophiolite, South Tianshan, China. *Annual Review of Earth and Planetary Sciences* **14**, 43–51.